5968 *Inorg. Chem.* **1998,** *37,* 5968−5969

Isolation and Structure of the First Azo Anion Radical Complexes of Ruthenium

Maya Shivakumar, Kausikisankar Pramanik, Prasanta Ghosh, and Animesh Chakravorty*

Department of Inorganic Chemistry, Indian Association for the Cultivation of Science, Calcutta 700 032, India

Received June 23, 1998

Among catenated nitrogen compounds, N−N bond orders of 1 and 2 are common as in hydrazines and azo compounds, respectively. In azo anion radicals (AAR) formed by the addition of an electron to the azo π^* orbital, eq 1

$$\underset{(\sigma^2\pi^2)}{-N{=}N-} + e \rightarrow \underset{(\sigma^2\pi^2\pi^{*1})}{-N\overset{\cdot\cdot}{-}N-^{-}} \qquad (1)$$

the formal bond order is 1.5. AAR species have been documented in solution,[1−4] but none has been isolated in pure form either in the free or in the coordinated state. This has been achieved in the present work,[5] thus providing an experimental measure of the AAR N−N length. The relevant azo ligands, complexes, and their abbreviations are set out in Chart 1. The reaction of 2-(arylazo)pyridines of type **1**[6] with **2**[7] has afforded the green crystalline AAR complexes of type **3** in excellent yields.[8] The solids are indefinitely stable in dry air, but solutions undergo facile aerial oxidation affording red-colored species of type $\mathbf{3}^+$ which have been isolated as PF_6^- salts[9] (the $E_{1/2}$ values of the $\mathbf{3}^+$/**3** couples lie in the range −0.3 to −0.4 V vs SCE). The type **3** complexes are paramagnetic (μ_{eff}: **3a**, 1.79 μ_B; **3b**, 1.75 μ_B), and their EPR spectra (Figure 1) consist of a strong line at $g = 2.000$ (for both **3a** and **3b**), the peak-to-peak line widths being 20−24 G. This result taken collectively with bond parameters reported below confirms the AAR description of **3**. AAR being a π-radical, the ^{14}N hyperfine splitting is small and is not resolved in EPR (Figure 1) as in other cases.[2,3] The $\mathbf{3}^+$ complexes are diamagnetic and afford well-resolved ^1H NMR lines.[9]

Chart 1

1a 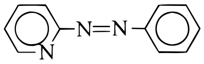 (pap)

1b 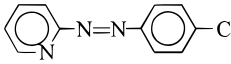 (Clpap)

2 $Ru^{II}(H)(Cl)(CO)(PPh_3)_3$

3a $Ru^{II}(pap^{\bullet -})(Cl)(CO)(PPh_3)_2$

3b $Ru^{II}(Clpap^{\bullet -})(Cl)(CO)(PPh_3)_2$

3a⁺ $Ru^{II}(pap)(Cl)(CO)(PPh_3)_2{}^+$

3b⁺ $Ru^{II}(Clpap)(Cl)(CO)(PPh_3)_2{}^+$

4 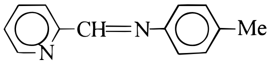 (pal)

5 $Ru^{II}(pal)(H)(Cl)(CO)(PPh_3)$

In the X-ray structures[10] of **3a** and $\mathbf{3b}^+$ $PF_6^-\cdot 2CH_2Cl_2$, the two RuN_2ClCP_2 coordination spheres have the same gross geometry (Figures 1 and 2). We have here a unique opportunity for (i) comparing the azo and AAR N−N lengths in the same environment and (ii) assessing the effect of AAR formation on other bond parameters. In uncoordinated azo compounds and hydrazines, the N−N distances are 1.25[11] and 1.45 Å,[12] respectively.

---

(1) Sadler, J. L.; Bard, A. J. *J. Am. Chem. Soc.* **1968**, *90*, 1979.

(2) Pal, C. K.; Chattopadhyay, S.; Sinha, C. R.; Chakravorty, A. *Inorg. Chem.* **1994**, *33*, 6140.

(3) Pal, C. K.; Chattopadhyay, S.; Sinha, C. R.; Chakravorty, A. *Inorg. Chem.* **1996**, *35*, 2442.

(4) Krause, R. A.; Krause, K. *Inorg. Chem.* **1984**, *23*, 2195.

(5) Extracted in part from the Ph.D. Thesis of Pramanik, K., Jadavpur University, Calcutta 700 032, India, September 1997, and presented in part in Indo-Russian Symposium, Nizhnii, Novogorod, September 1993.

(6) (a) Krause, R. A.; Krause, K. *Inorg. Chem.* **1980**, *19*, 2600. (b) Goswami, S.; Chakravarty, A. R.; Chakravorty, A. *Inorg. Chem.* **1981**, *20*, 2246. (c) Ghosh, B. K.; Chakravorty, A. *Coord. Chem. Rev.* **1989**, *95*, 239. (d) Kakoti, M.; Deb, A. K.; Goswami, S. *Inorg. Chem.* **1992**, *31*, 1302. (e) Santra, B. K.; Thakur, G. A.; Ghosh, P.; Pramanik, A.; Lahiri, G. K. *Inorg. Chem.* **1996**, *35*, 3050. (f) Misra, T. K.; Das, D.; Sinha, C. R.; Ghosh, P.; Pal, C. K. *Inorg. Chem.* **1998**, *37*, 1672 and references therein.

(7) Ahmad, N.; Levison J. J.; Robinson, S. D.; Uttley, M. F. *Inorg. Synth.* **1975**, *15*, 45.

(8) **3a**: To an excess of **1a** (60 mg, 0.33 mmol) in dry heptane (25 mL) was added **2** (100 mg, 0.10 mmol), and the mixture was heated to reflux in a nitrogen atmosphere for 1 h. The dark green crystalline complex precipitated in 70% yield on cooling. Data for **3a** are as follows. Anal. Calcd (found) for $C_{48}H_{39}N_3OP_2ClRu$: C, 65.85 (66.08); H, 4.32 (4.47); N, 4.91 (4.82). UV−vis (C_6H_6) [λ_{max}, nm (ϵ, M^{-1} cm^{-1})]: 580 (5400), 460 (4200), 370 (15 000). IR (KBr, cm^{-1}): 1290 (ν_{N-N}), 1923 (ν_{C-O}), 310 (ν_{Ru-Cl}). **3b** was similarly prepared in 80% yield from **1b** and **2**. Data for **3b** are as follows. Anal. Calcd (found) for $C_{48}H_{38}N_3OP_2Cl_2Ru$: C, 62.76 (63.57); H, 4.24 (4.19); N, 4.85 (4.63). UV−vis (C_6H_6) [λ_{max}, nm (ϵ, M^{-1} cm^{-1})]: 570 (5500), 455 (4100), 370 (15 000). IR (KBr, cm^{-1}): 1288 (ν_{N-N}), 1923 (ν_{C-O}), 320 (ν_{Ru-Cl}).

(9) $\mathbf{3a}^+$: To a solution of **3a** (50 mg, 0.06 mmol) in dichloromethane (20 mL) was added NH_4PF_6 (20 mg, 0.12 mmol in 5 mL acetonitrile), and the mixture was magnetically stirred for 2 h. The red solution was dried under reduced pressure, washed with water, and dried in vacuo. Subsequent chromatographic workup of a dichloromethane solution on silica gel (eluent 1:4 acetonitrile−benzene) afforded red-colored $\mathbf{3a}^+$ PF_6^- in 70% yield. Data for $\mathbf{3a}^+$ PF_6^- are as follows. Anal. Calcd (found) for $C_{48}H_{39}N_3OF_6P_3ClRu$: C, 56.35 (56.67); H, 3.71 (3.84); N, 3.89 (4.13). UV−vis (CH_2Cl_2) [λ_{max}, nm (ϵ, M^{-1} cm^{-1})]: 500 (2400), 450 (2600), 380 (9800). IR (KBr, cm^{-1}): 1340 (ν_{N-N}), 1960 (ν_{C-O}), 330 (ν_{Ru-Cl}). ^1H NMR ($CDCl_3$, 298 K, ppm from TMS): δ 8.75 (d, J = 7.8, 1H), 8.27 (t, J = 7.7, 1H), 7.81 (d, J = 5.1, 1H), 6.94 (t, J = 8.0, 2H), 6.78 (t, J = 6.6, 1H), 6.75 (d, J = 8.1, 2H). $\mathbf{3b}^+$ was similarly prepared from **3b** and was isolated as $\mathbf{3b}^+$ PF_6^-. Data for $\mathbf{3b}^+$ PF_6^- are as follows. Anal. Calcd (found) for $C_{48}H_{38}N_3OF_6P_3Cl_2Ru$: C, 54.36 (54.80); H, 3.74 (3.61); N, 3.68 (3.99). UV−vis (CH_2Cl_2) [λ_{max}, nm (ϵ, M^{-1} cm^{-1})]: 505 (2500), 460 (2800), 390 (9800). IR (KBr, cm^{-1}): 1330 (ν_{N-N}), 1945 (ν_{C-O}), 330 (ν_{Ru-Cl}). ^1H NMR ($CDCl_3$, 298 K, ppm from TMS): δ 8.75 (d, J = 9.0, 1H), 8.23 (t, J = 7.5, 1H), 7.81 (d, J = 3.0, 1H), 6.89 (t, J = 9.0, 2H), 6.78 (t, J = 6.0, 1H), 6.65 (d, J = 9.0, 2H).

(10) A Siemens R3m/V four-circle diffractometer equipped with a graphite crystal monochromator and Mo Kα (λ = 0.710 73 Å) radiation was used to collect data. The structures were solved by the Patterson heavy-atom method (SHELXTL-V 5.03) and refined on F^2 by full matrix least squares using all unique data. All non-hydrogen atoms for **3a** and $\mathbf{3b}^+$ PF_6− $\cdot 2CH_2Cl_2$ were anisotropically refined with H atoms included in calculated positions (riding model). Data for **3a**: monoclinic $P2_1/n$ (No. 14), a = 17.244(9) Å, b = 11.047(4) Å, c = 22.076(7) Å, β = 97.28(4)°, V = 4171(3) Å^3, Z = 4; R1 = 0.0612, wR2 = 0.1072 for reflections with $I > 2\sigma(I)$. Data for $\mathbf{3b}^+$ $PF_6^-\cdot 2CH_2Cl_2$: orthorhombic *Pbca* (No. 61), a = 15.041(7) Å, b = 23.986(8) Å, c = 28.940(20) Å, V = 10442(9) Å^3, Z = 8; R1 = 0.0600, wR2 = 0.1346 for reflections with $I > 2\sigma(I)$.

(11) (a) Mostad, A.; Romming, C. *Acta Chem. Scand.* **1971**, *25*, 3561. (b) Chang, C. H.; Porter, R. F.; Brauer, S. H. *J. Am. Chem. Soc.* **1970**, *92*, 5313. (c) Roy, T.; Sengupta, S. P. *Cryst. Struct. Commun.* **1980**, *9*, 965.

(12) Morino, Y.; Iijima, T.; Murata, Y. *Bull. Chem. Soc. Jpn.* **1960**, *33*, 46.

10.1021/ic980719w CCC: $15.00

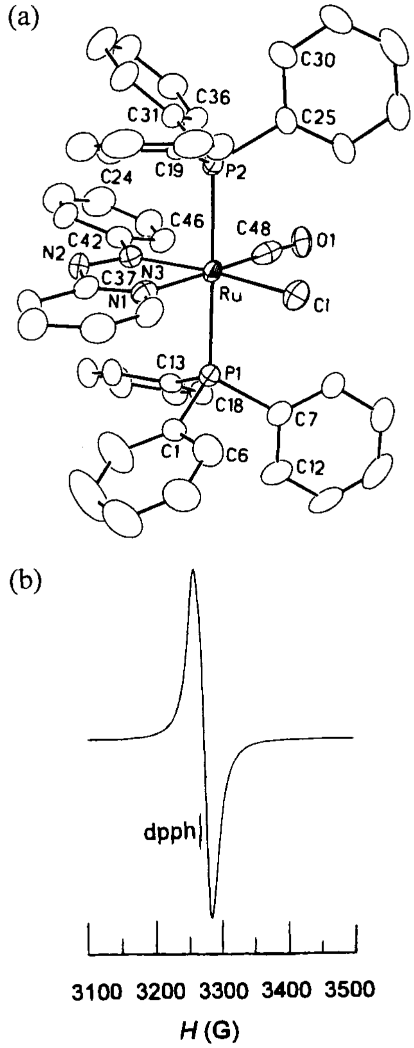

Figure 1. (a) Molecular structure of [Ru(pap$^{\bullet-}$)(Cl)(CO)(PPh$_3$)$_2$] (**3a**) (30% thermal ellipsoids). Selected bond distances (Å) and angles (deg): Ru−Cl, 2.440(2); Ru−P(1), 2.416(2); Ru−P(2), 2.400(2); Ru−N(1), 2.154(6); Ru−N(3), 2.087(6); Ru−C(48), 1.856(10); N(2)−N(3), 1.333(7); O(1)−C(48), 1.091(9); P(1)−Ru−P(2), 178.79(7); Cl−Ru−N(3), 164.8(2); N(1)−Ru−C(48), 179.3(3); N(1)−Ru−N(3), 76.4(2); Ru−C(48)−O(1), 172.5(7). (b) Powder EPR spectrum of **3a** in the X-band (9.11 GHz) at 298 K. Instrument settings: power, 30 dB; modulation, 100 kHz; sweep center, 3300 G; sweep width, 1000 G; sweep time, 240 s.

In **3a** the distance has an intermediate value, 1.333(7) Å. A plot of N−N bond order versus bond length in the range N−N, N$\overset{\cdots}{-}$N, and N=N is in Figure 2b.

In **3b**$^+$, the N−N distance is still 0.04 Å longer than 1.25 Å due to the strong t$_2 \rightarrow \pi^*$(azo) back-bonding.[6a−c,13,14] In the plot of Figure 2b, the length in **3b**$^+$ corresponds to a bond order of 1.7. Back-bonding to π^*(azo) is expected to become unimportant upon AAR formation, and there is indeed a 0.04 Å increase in the Ru−N3 distance between **3b**$^+$ and **3a**. The CO and PPh$_3$ ligands play a stabilizing role by contributing more to back-bonding in **3a** than in **3b**$^+$, as can be seen in bond length data and in ν_{CO} values[8,9] (a 35 cm^{-1} decrease between **3**$^+$ and **3**). The trans influence of the AAR site on the Ru−Cl length and ν_{Ru-Cl}[8,9] is also noteworthy.

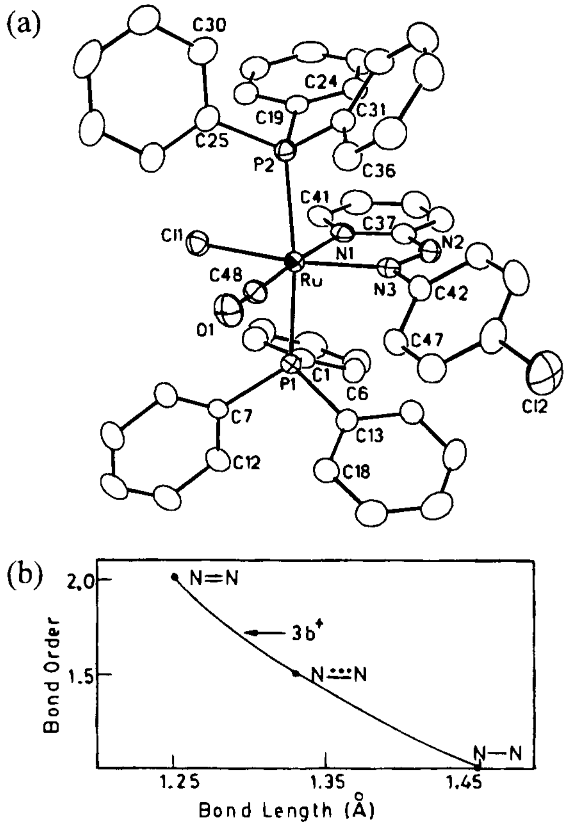

Figure 2. (a) Molecular structure of [Ru(Clpap)(Cl)(CO)(PPh$_3$)$_2$]$^+$ (**3b**$^+$) showing 30% probability ellipsoids. Selected bond distances (Å) and angles (deg): Ru−Cl(1), 2.391(2); Ru−P(1), 2.429(2); Ru−P(2), 2.420(2); Ru−N(1), 2.125(5); Ru−N(3), 2.042(5); Ru−C(48), 1.874(8); N(2)−N(3), 1.293(7); O(1)−C(48), 1.126(8); P(1)−Ru−P(2), 170.79(6); Cl(1)−Ru−N(3), 166.8(2); N(1)−Ru−C(48), 174.8(2); N(1)−Ru−N(3), 75.8(2); Ru−C(48)−O(1), 178.0(6). (b) A plot of bond order versus bond length (Å).

Finally, a scrutiny of our synthetic procedure, eq 2, is in order. The key to our success in the isolation of AAR

$$\mathbf{1} + \mathbf{2} \rightarrow \mathbf{3} + {}^{1}/_{2}\mathrm{H}_2 + \mathrm{PPh}_3 \qquad (2)$$

species of type **3** lies in the choice of **2** as starting material ensuring (i) in situ availability of the required (eq 1) reducing equivalent via Ru−H bond cleavage, eq 2, and (ii) a stabilizing environment of π-acid ligands (CO, PPh$_3$). The role of Ru−H bond cleavage in AAR formation is further highlighted in the reaction of **2** with the aldimine pal,[15] **4**. The aldimine π^* orbital lies too high for anion radical formation, and here the product obtained is **5**, in which the Ru−H bond is preserved, as proved by the ^{1}H NMR doublet (coupling with ^{31}P) at $\sim -12\ \delta$.[16]

Acknowledgment. We are thankful to the Indian National Science Academy, Department of Science and Technology, and the Council of Scientific and Industrial Research, New Delhi, for financial support. Affiliation with the Jawaharlal Nehru Centre for Advanced Scientific Research, Bangalore, is acknowledged.

Supporting Information Available: An X-ray crystallographic file, in CIF format, is available on the Internet only. Access information is given on any current masthead page.

IC980719W

---

(13) (a) Krause, R. A.; Krause, K. *Inorg. Chem.* **1982**, *21*, 1714. (b) Goswami, S.; Mukherjee, R.; Chakravorty, A. *Inorg. Chem.* **1983**, *22*, 2825.

(14) (a) Seal, A.; Ray, S. *Acta Crystallogr.* **1984**, *C40*, 929. (b) Krause, K.; Krause, R. A.; Larsen, S.; Rasmussen, B. *Acta Chem. Scand., Ser. A* **1985**, *A39*, 375.

(15) Bähr, V. G.; Thämlitz, H. *Z. Anorg. Allg. Chem.* **1955**, *282*, 3.

(16) Details of spectroscopic and X-ray structural characterization of **5** will be presented elsewhere.